

A study on different failure criteria to predict damage in glass/polyester composite beams under low velocity impact

Manizheh Aghaei^a, Mohammad R. Forouzan^{*},
Mehdi Nikforouz^b and Elham Shahabi^c

Department of mechanical engineering, Isfahan University of Technology, Iran

(Received May 21, 2014, Revised September 30, 2014, Accepted November 23, 2014)

Abstract. Damage caused by low velocity impact is so dangerous in composites because although in most cases it is not visible to the eye, it can greatly reduce the strength of the composite material. In this paper, damage development in U-section glass/polyester pultruded beams subjected to low velocity impact was considered. Different failure criteria such as Maximum stress, Maximum strain, Hou, Hashin and the combination of Maximum strain criteria for fiber failure and Hou criteria for matrix failure were programmed and implemented in ABAQUS software via a user subroutine VUMAT. A suitable degradation model was also considered for reducing material constants due to damage. Experimental tests, which performed to validate numerical results, showed that Hashin and Hou failure criteria have better accuracy in predicting force-time history than the other three criteria. However, maximum stress and Hashin failure criteria had the best prediction for damage area, in comparison with the other three criteria. Finally in order to compare numerical model with the experimental results in terms of extent of damage, bending test was performed after impact and the behavior of the beam was considered.

Keywords: failure criteria; damage modes; glass/polyester composite; ABAQUS/Explicit; VUMAT

1. Introduction

In recent years, the usage of composite materials has grown remarkably, as well as the field of their application. Composite materials like PMCs (Polymer Matrix Composites) are nowadays competing with conventional materials such like metals, because they have different and some beneficial chemical and physical properties. Beneficial properties are high specific strength, high specific stiffness, high specific toughness, corrosion resistance, wear resistance, chemical resistance, thermal insulation, electrical insulation, acoustic insulation, reduced manufacturing and

*Corresponding author, Associate Professor, E-mail: forouzan@cc.iut.ac.ir

^a Graduated M.Sc., E-mail: manizheh.aghaei@me.iut.ac.ir

^b Ph.D. Student, E-mail: m.nikforouz@me.iut.ac.ir

^c Ph.D. Student, E-mail: e.shahabi@me.iut.ac.ir

maintenance costs, producing complex shapes with improved properties in the desired directions, etc. Some research effort is needed to explore the beneficial properties of composite materials and understand their mechanical properties. For example, the modeling of mechanical properties of composite materials is much more complicated than that for Metals. In particular, the heterogeneous nature of composites causes difficulties to assess their failure. There thus exists a variety of failure criteria that confused potential users of composite materials. Different failure criteria are dealt with in the literature either as static or as dynamic loading. In a recent studies of static loading Irhirane *et al.* (2010) tested the accuracy of different failure criteria via simulation of damage in three-point bending tests. Icardi *et al.* (2007) compared predictions of different failure theories for plates differing in thicknesses under central point loading. In dynamic loadings, Garnich and Akula (2008) reviewed the effect of different degradation models to predict damage in a composite material. Donadon *et al.* (2008) used Maximum strain and Puck failure criteria with energy based degradation method to model low velocity impact damage. The same authors also applied different failure criteria with a new kind of energy based degradation model to simulate damage in carbon-epoxy specimens under tensile loading (Donadon *et al.* 2009).

One disadvantage of PMCs is their vulnerability to impact loads that cause internal damages. These are generally not visible, but decrease the load carrying capability of the material. Composite structures may either intentionally or accidentally be subjected to high impact loads. In recent decades, the prediction of damage of composite plates and beams under impact played a central role. Sutherland and Guedes Soares (2005) investigated damage caused by low velocity impact on glass polyester plates with low fiber contents. They studied the effect of laminate thickness and fiber crimp on failure modes of low velocity impact damage. Menna *et al.* (2011) used orthotropic failure criteria combined with strength based failure criteria to model different modes of damage including delamination due to low velocity impact. Johnson *et al.* (2006) compared the accuracy of different failure criteria in modeling impact damage of large and small scale composite plates. Tiberkak *et al.* (2008) studied the effect of 90° plies percentage on damage in low velocity impact and to obtain the velocities at which matrix cracking initiated. Khalili *et al.* (2011) examined the effect of different parameters such as element type and meshing pattern to model low velocity impact.

To date, most researchers worked on composite plates subjected to low velocity impact, while few studies investigate impact on composite structural members such as beams. Santiuste *et al.* (2010) used Hou and Hashin failure criteria to model the damage of composite laminated beams under dynamic bending. They used different carbon-epoxy laminated beams in order to validate their numerical model. Sanchez-Saez *et al.* (2007) studied the dynamic flexural behavior of composite beams at low temperature. Minak *et al.* (2009) investigated the behavior of carbon-epoxy composite tubes under low velocity and low energy impact.

In the current work different failure criteria such as Maximum stress, Maximum strain, Hou, Hashin and the combination of Maximum strain failure criteria for fiber failure and Hou criteria for matrix failure are written in a user subroutine (VUMAT) and are implemented in ABAQUS/Explicit software. Experimental tests were performed to validate numerical model. Subsequently the respective precision of these criteria to detect damage of composite pultruded beams caused by low velocity impact is investigated. Finally, the best failure criteria to predict the peak impact force will be identified and different failure criteria predicting the damage zones will be compared. At the end in order to compare numerical model with the experimental results in terms of extent of damage, bending test was performed after impact and the behavior of the beam was considered.

2. Problem formulation

2.1 Failure criteria

Failure criteria can be divided into two main categories: ‘mode dependent’ and ‘mode independent’ criteria.

Table 1 Maximum stress, maximum strain, Hashin and Hou failure criteria

Mode	Maximum stress	Maximum strains	Hashin	Hou
FTF ^a	$\sigma_{11} \geq X_t$	$\varepsilon_{11} \geq Ex_t$	$\left(\frac{\sigma_{11}}{X_t}\right)^2 + \left(\frac{\sigma_{12}^2 + \sigma_{13}^2}{S_{12}^2}\right) \geq 1$	$\left(\frac{\sigma_{11}}{X_t}\right)^2 + \left(\frac{\sigma_{12}^2 + \sigma_{13}^2}{S_{12}^2}\right) \geq 1$
FCF ^b	$ \sigma_{11} \geq X_c$	$ \varepsilon_{11} \geq Ex_c$	$ \sigma_{11} \geq X_c$	$\left(\frac{\sigma_{11}}{X_c}\right)^2 + \left(\frac{\sigma_{12}^2 + \sigma_{13}^2}{S_{12}^2}\right) \geq 1$
MTF ^c	$\sigma_{22} \geq Y_t$	$\varepsilon_{22} \geq Et_t$	$\frac{1}{Y_t^2}(\sigma_{22} + \sigma_{33})^2$ $+ \frac{1}{S_{23}^2}(\sigma_{23}^2 - \sigma_{22}\sigma_{33})$ $+ \frac{1}{S_{12}^2}(\sigma_{12}^2 - \sigma_{13}^2) \geq 1$	$\left(\frac{\sigma_{22}}{Y_t}\right)^2 + \left(\frac{\sigma_{12}}{S_{12}}\right)^2 + \left(\frac{\sigma_{23}}{S_{23}}\right)^2 \geq 1$
			(for $(\sigma_{22} + \sigma_{33}) > 0$)	
MCF ^d	$ \sigma_{22} \geq Y_c$	$ \varepsilon_{22} \geq Ey_c$	$\frac{1}{Y_c} \left[\left(\frac{Y_c}{2S_{23}} \right)^2 - 1 \right] (\sigma_{22} + \sigma_{33})$ $+ \frac{1}{4S_{23}^2}(\sigma_{22} + \sigma_{33})^2$ $+ \frac{1}{S_{23}^2}(\sigma_{23}^2 - \sigma_{22}\sigma_{33})$ $+ \frac{1}{S_{12}^2}(\sigma_{12}^2 + \sigma_{13}^2) \geq 1$	$\frac{1}{4} \left(\frac{-\sigma_{22}}{S_{12}} \right)^2 + \frac{Y_c^2 \sigma_{22}}{4S_{12}^2 Y_c}$ $- \frac{\sigma_{22}}{Y_c} + \left(\frac{\sigma_{12}}{S_{12}} \right)^2 \geq 1$
			(for $(\sigma_{22} + \sigma_{33}) < 0$)	

^a Fiber tensile failure

^b Fiber compressive failure

^c Matrix tensile failure

^d Matrix compressive failure

Mode independent failure theories use a polynomial expression in terms of either stresses or strains to evaluate damage without distinguishing between different modes of damage. The most famous criterion of this kind is Tsi-Wu criterion, which in the generalized form is as Eq. (1).

$$F_i \sigma_i + F_{ij} \sigma_i \sigma_j + F_{ijk} \sigma_i \sigma_j \sigma_k \geq 1 \quad i, j, k = 1, 2, \dots, 6 \quad (1)$$

Where F_i , F_{ij} , F_{ijk} are strength coefficient tensors and $\sigma_{i,j,k}$ ($i, j, k = 1, 2, \dots, 6$) are normal and shear stress components.

Mode dependent failure criteria, which are used in this work, can distinguish between different modes of failure such as fiber breakage, fiber buckling, matrix cracking and matrix crushing. In the present work Maximum stress, Maximum strain, Hashin, Hou and the combination of Maximum strain failure criteria for fiber failure and Hou criteria for matrix failure, have been used and are presented in Table 1. The failure modes are fiber tensile failure (FTF), fiber compressive failure (FCF), matrix tensile failure (MTF) and matrix compressive failure (MCF).

Maximum stress and Maximum strain criteria are ‘non-interactive’ criteria since considering single stress or strain components in each mode. Hou and Hashin failure criteria however, are known as ‘interactive’ criteria for considering an interaction of different stress components in each mode.

Hou criteria which are based on the well-known Chang-Chang criteria (Chang and Chang 1987) are the latest among those four failure criteria. They were used in (Cui *et al.* 2009) to investigate impact damage and the residual tensile strength after impact loading in composite laminates under low velocity impact and give good results. However, Hashin criteria are the most popular criteria among the criteria selected in this paper and have been applied by many researchers such as Sanchez-Saez *et al.* (2007) and Batra *et al.* (2012). Maximum stress and Maximum strain criteria are also frequently used because of their simplicity (literature).

2.2 Material degradation model

In damage mechanics, when the failure criterion satisfies, elastic properties should be degraded due to damage either instantaneously or gradually. In this paper an instantaneous material degradation model based on Tan and Perez model (Tan and Perez 1993) is used as is listed in Table 2.

Using this degradation model the so called ‘reduced stress’ is determined by Eq. (2).

$$\sigma^{red} = C^d \varepsilon \quad (2)$$

Table 2 Material degradation model

Damage mode	Property degradation rule
FTF	$E_{11}^d = 0.07 E_{11}$
FCF	$E_{11}^d = 0.14 E_{11}$
MTF	$E_{22}^d = 0.2 E_{22}$, $G_{12}^d = 0.2 G_{12}$, $G_{23}^d = 0.2 G_{23}$
MCF	$E_{22}^d = 0.4 E_{22}$, $G_{12}^d = 0.4 G_{12}$, $G_{23}^d = 0.4 G_{23}$

In which the matrix C^d is obtained by replacing the degraded elastic properties of the material according to the failure mode in the stiffness matrix C . For an orthotropic material the stiffness matrix is defined as in Eq. (3).

$$\begin{Bmatrix} \sigma_{11} \\ \sigma_{22} \\ \sigma_{33} \\ \sigma_{12} \\ \sigma_{23} \\ \sigma_{13} \end{Bmatrix} = \begin{bmatrix} C_{11} & C_{12} & C_{13} & 0 & 0 & 0 \\ C_{12} & C_{22} & C_{23} & 0 & 0 & 0 \\ C_{13} & C_{23} & C_{33} & 0 & 0 & 0 \\ 0 & 0 & 0 & C_{44} & 0 & 0 \\ 0 & 0 & 0 & 0 & C_{55} & 0 \\ 0 & 0 & 0 & 0 & 0 & C_{66} \end{bmatrix} \begin{Bmatrix} \varepsilon_{11} \\ \varepsilon_{22} \\ \varepsilon_{33} \\ \gamma_{12} \\ \gamma_{23} \\ \gamma_{13} \end{Bmatrix} = C \varepsilon \quad (3)$$

where :

$$C_{11} = E_{11}(1 - \vartheta_{23}\vartheta_{32})/\vartheta$$

$$C_{22} = E_{22}(1 - \vartheta_{13}\vartheta_{31})/\vartheta$$

$$C_{33} = E_{33}(\vartheta_{12} + \vartheta_{32}\vartheta_{13})/\vartheta$$

$$C_{12} = E_{22}(\vartheta_{12} - \vartheta_{32}\vartheta_{13})/\vartheta$$

$$C_{23} = E_{22}(\vartheta_{23} - \vartheta_{21}\vartheta_{13})/\vartheta$$

$$C_{13} = E_{22}(\vartheta_{13} - \vartheta_{12}\vartheta_{23})/\vartheta$$

$$C_{44} = G_{12}$$

$$C_{55} = G_{23}$$

$$C_{66} = G_{13}$$

$$\vartheta_{21} = E_{22}\vartheta_{12} + E_{11}$$

$$\vartheta_{32} = E_{33}\vartheta_{23} + E_{22}$$

$$\vartheta_{31} = E_{33}\vartheta_{13} + E_{11}$$

$$\vartheta = 1 - \vartheta_{12}\vartheta_{21} - \vartheta_{23}\vartheta_{32} - \vartheta_{13}\vartheta_{31} - 2\vartheta_{32}\vartheta_{21}\vartheta_{13}$$

In which E_{ij} , ϑ_{ij} are the orthotropic components of elastic modulus and Poisson ratio respectively.

The above mentioned degradation model is a ‘stiffness degradation model’. It can simply be converted to the form of ‘stress degradation’ which is more suitable to be implemented in the user

Table 3 Material properties provided by the manufacturer

Material properties	Value	Material properties	Value	Material properties	Value
E_{11}	30 Gpa	X_T	460 Mpa	Ex_t	0.0136 mm
$E_{22} = E_{33}$	8 Gpa	X_C	420 Mpa	Ex_c	0.0126 mm
$G_{12} = G_{13}$	3 Gpa	$Y_t = Z_t$	75 Mpa	Ey_t	0.0026 mm
G_{23}	3 Gpa	$Y_c = Z_c$	62 Mpa	Ey_c	0.0017 mm
$\vartheta_{12} = \vartheta_{13}$	0.35	$S_{12} = S_{13}$	31 Mpa	Es_{12}	0.0103 mm
ϑ_{23}	0.15	S_{23}	37 Mpa	ρ	1.86E-9 Ton/mm ³

subroutine VUMAT. Substituting $e = C^{-1}s$ into Eq. (2) obtained

$$\Rightarrow \sigma^{red} = D\sigma \quad (4)$$

$$D = C^d C^{-1} \quad (5)$$

With a little manipulation, D for each failure mode is obtained in the form of Eq. (6)

$$D = \begin{bmatrix} (1-d_f) & 0 & 0 & 0 & 0 & 0 \\ 0 & (1-d_m) & 0 & 0 & 0 & 0 \\ 0 & 0 & (1-d_m) & 0 & 0 & 0 \\ 0 & 0 & 0 & (1-d_m) & 0 & 0 \\ 0 & 0 & 0 & 0 & (1-d_m) & 0 \\ 0 & 0 & 0 & 0 & 0 & 1 \end{bmatrix} \quad (6)$$

with : $d_{ft} = 0.93$, $d_{fc} = 0.86$, $d_{mt} = 0.8$, $d_{mc} = 0.6$

In which the damage parameters d_{ft} , d_{fc} , d_{mt} , d_{mc} are state variables for fiber tensile, fiber compressive, matrix tensile and matrix compressive failure modes respectively. These parameters are obtained with Eq. (5) by inserting material properties, which are summarized in Table 3, in the components of matrices C and C^d .

2.3 Finite element model

Dimensions of beam section and the assembly of beam, projectile and support fixtures are shown in Fig. 1. The length of the beam is 250 mm. The contact condition between the beam and projectile as well as the contact between the beam and Support fixtures is defined to be hard contact for normal behavior and frictional contact with the coefficient of 0.2 for tangential behavior.

Three dimensional mesh was used with fine elements in the center of the beam where the impact occurred, as is shown in Fig. 2. Mesh sensitivity analysis was conducted by successive

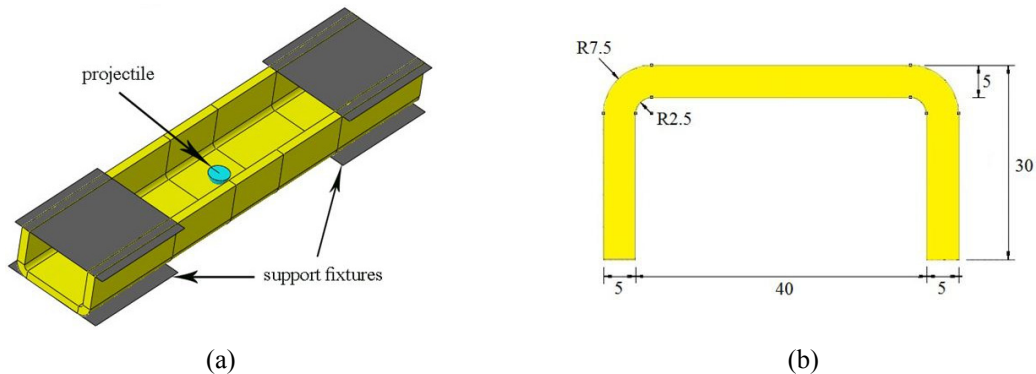


Fig. 1 (a) Simulation of the test, including support fixtures and projectile; (b) Beam section dimensions in mm

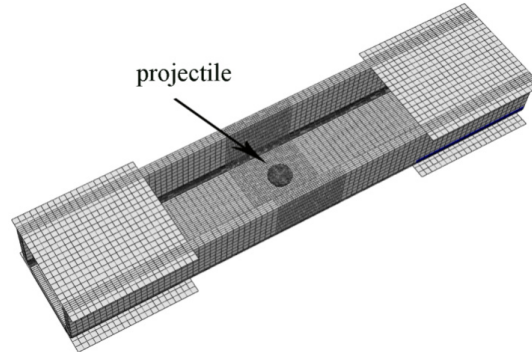


Fig. 2 Mesh configuration of the beam

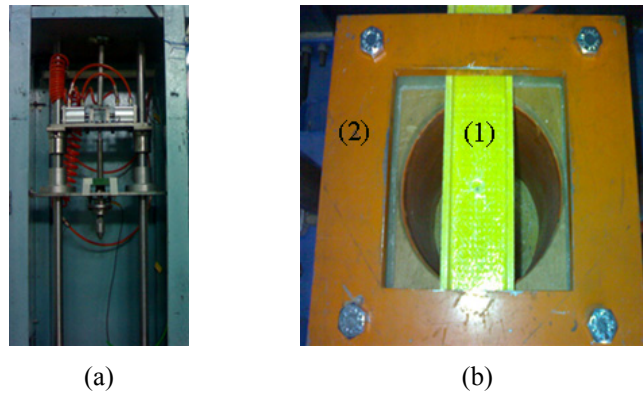


Fig. 3 (a) Drop-weight tower; (b) (1) beam; and (2) support fixtures

mesh refinement. The final mesh had 78000 8-node brick elements using reduced integration and hourglass control (C3D8R in ABAQUS notation), with five elements along the thickness. Support fixtures and hemispherical projectile was modeled as rigid bodies using 4-node 3-D bilinear rigid quadrilateral elements (R3D4 in ABAQUS notation) because they were much stiffer than the composite beam.

Damage criteria, damage evolution law and stress updating were defined in VUMAT subroutine.

3. Experiment

The specimens used in this study are U-section pultruded beams, made up of E-glass fibers of type tex4800 and isophthalic polyester resin. These beams are made up of a unidirectional layer in the center of beam which is sandwiched between layers of continuous strand mats (CSM). The material properties for the composite beam provided by the manufacturer as summarized in Table 3. Fig. 3(a) shows the beam and its support of the impact test. Low velocity impact tests were performed by impact testing machine shown in Fig. 3(b). The diameter of hemispherical projectile

was 11.6 mm and the dropping height and mass were 66 cm and 7.5 kg respectively.

4. Results and discussion

4.1 Force-time curve

Force history diagram obtained from different failure criteria are shown in Fig. 4. The result of the experiment is shown by solid line. The oscillations in the diagram are due to the wave return from the foundation to the beam and the overall trend of the diagram is of interest.

In the ascending part of the diagram Hou and Hashin failure criteria have better agreement with experimental result because of better prediction of the peak force of the impact. Maximum stress, Maximum strain and Hou-Maximum strain criteria predict the moment of the peak force well, but peak force is predicted to be higher than in reality. But in general, all the criteria predict the behavior of the beam with a good approximation because maximum 15% error occurred in predicting peak force for maximum stress failure criteria in comparison with experiment while this error is just 0.8% for Hou failure criteria.

In the descending part of the diagram, the simulation does not follow the trend of experimental

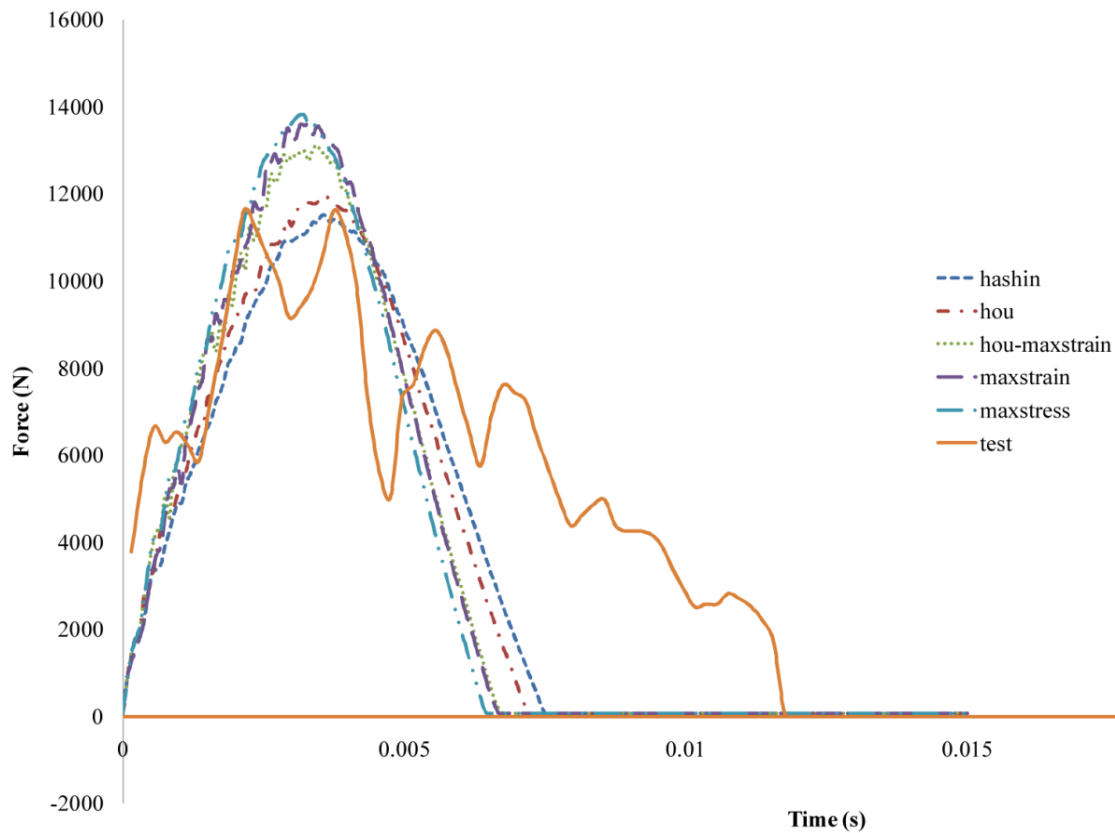


Fig. 4 Simulation and experimental force-time curve for low velocity impact

results. This discrepancy between simulation and experiment might be due to non-rigid behavior of the machine foundation toward the impact. However, peak force is the most serious consequence of the impact and this discrepancy is of little practical significance.

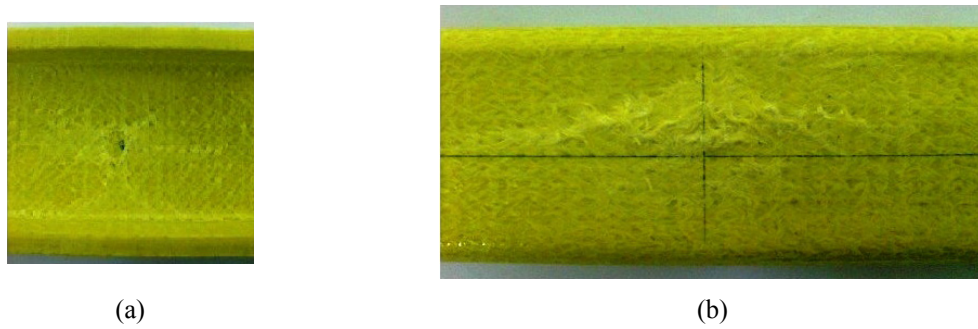


Fig. 5 Damaged zone under low velocity impact: (a) impact face; (b) opposite to the impact face

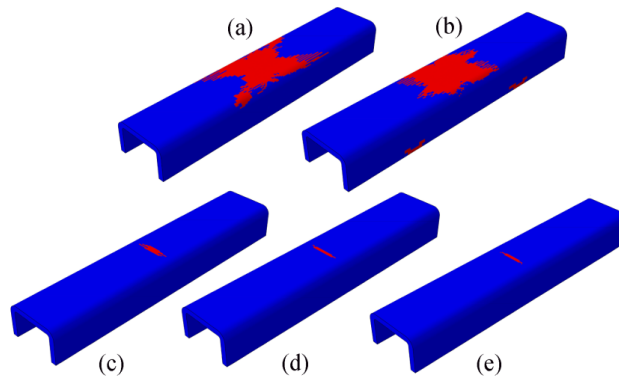


Fig. 6 Predicted damage in fiber tensile failure (FTF) mode: (a) Hashin; (b) Hou; (c) Maximum stress; (d) Maximum strain; (e) Maximum strain-Hou

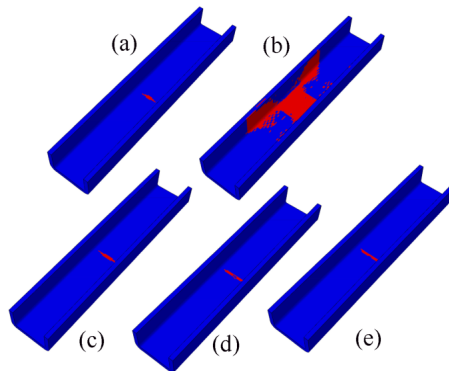


Fig. 7 Predicted damage in fiber compressive failure (FCF) mode: (a) Hashin; (b) Hou; (c) Maximum stress; (d) Maximum strain; (e) Maximum strain-Hou

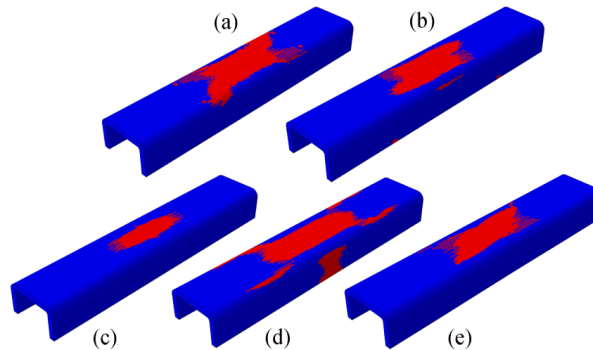


Fig. 8 Predicted damage in matrix tensile failure (MTF) mode: (a) Hashin; (b) Hou; (c) Maximum stress; (d) Maximum strain; (e) Maximum strain-Hou

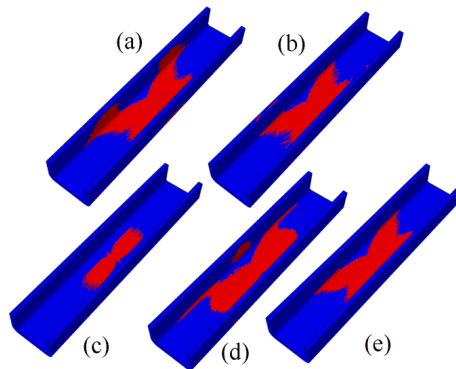


Fig. 9 Predicted damage in matrix compressive failure (MCF) mode: (a) Hashin; (b) Hou; (c) Maximum stress; (d) Maximum strain; (e) Maximum strain-Hou

4.2 Modes of failure

Fig. 5 represents the damage in both sides of the beam after impact test. Internal damage could not be seen exactly by the eye, but it can be predicted by simulation. In the following a detailed discussion of the predicted damaged zone by each failure criteria is presented.

Fiber tensile failures are shown in Fig. 6. Hou and Hashin failure criteria predict the extent of damage more than the other three criteria.

Fiber compressive failures can be seen in Fig. 7. Hou criteria predict the more extended damage zone for this mode of failure.

Matrix tensile failures are shown in Fig. 8. For Maximum strain criteria, damage can be seen not only in the web but also in the flanges of the beam.

Matrix compression failures are almost the same for all of the five criteria as can be seen in Fig. 9.

4.3 bending after impact

In order to compare the results of numerical model with the experiment, according to the features available, a technique was designed. According to this method, after the beam was

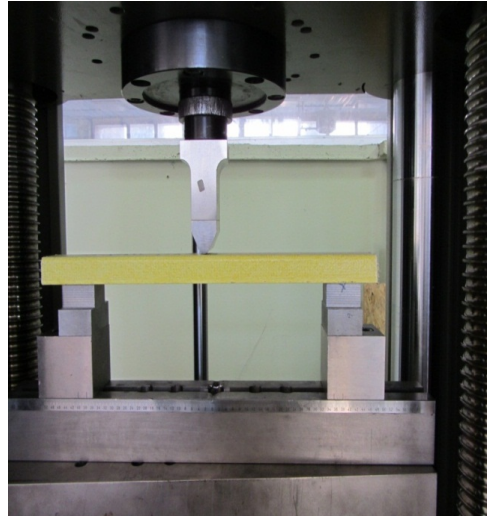


Fig. 10 Bending test after impact loading

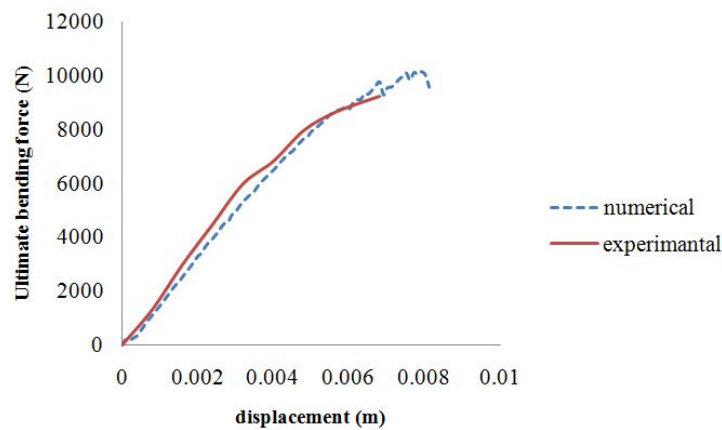


Fig. 11 Force displacement diagram for bending after impact for numerical and experimental model

impacted at the middle, it put under bending deflection and it's bending behavior after impact was compared for numerical and experimental model. The configuration of experimental set is shown in Fig. 10. Fig. 11 shows the results of experiment and simulation for force-displacement diagram. The simulation was done for Hou-Maximum strain criteria.

This figure shows good correlation between experiment and numerical model and ultimate bending force for numerical and experimental results are almost the same.

5. Conclusions

In this work, the failure of U-section glass/polyester pultruded beams in response to low velocity impacts was simulated by a FE model, implemented into ABAQUS/Explicit software. A

comparison between Maximum stress, Maximum strain, Hou, Hashin and Maximum strain-Hou failure criteria was carried out to predict the damage caused by low velocity impact. Experimental tests were performed to validate the numerical TE model. Hou and Hashin failure criteria faithfully predicted the peak force of the projectile, whereas peak force was overestimated by the other three criteria.

The extent of damage inflicted to the beam was evaluated by four failure modes considered in the present study, i.e., fiber tension failure (FTF), fiber compression failure (FCF), matrix tension failure (MTF) and matrix compression failure (MCF). In each mode, the damage predicted by five failure criteria was a little different. It is not easy to determine the true one by visual inspection even with naked eye (difficult to understand). One way to evaluate the extents of damage is post bending of the damaged beam and comparison of the results with that of intact beam which is the subject of a future paper. Finally in order to validate numerical model in terms of extent of damage a method was designed and bending test was performed after impact. It was seen that peak force was predicted close to experiment for maximum strain-Hou failure criteria and It can be concluded that for other criteria this correlation will be obtained because the extent of damage for all criteria was obtained almost the same in Section 4.2.

References

- Batra, R.C., Gopinath, G. and Zheng, J.Q. (2012), "Damage and failure in low energy impact of fiber-reinforced polymeric composite laminates", *Compos. Struct.*, **94**(2), 540-547.
- Chang, F. and Chang, K. (1987), "A progressive damage model for laminated composites containing stress concentrations", *Compos. Mater.*, **21**(9), 834-855.
- Cui, H., Wen, W. and Cui, H.T. (2009), "An integrated method for predicting damage and residual tensile strength of composite laminates under low velocity impact", *Comput. Struct.*, **87**(7-8), 456-466.
- Donadon, M.V., Iannucci, L., Falzon, B.G., Hodgkinson, J.M. and Almeida, S.F.M. (2008), "A progressive failure model for composite laminates subjected to low velocity impact damage", *Comput. Struct.*, **86**(11-12), 1232-1252.
- Donadon, M.V., Almeida, M., Arbelo, M.A. and Faria, A. (2009), "A three-dimensional ply failure model for composite structures", *Int. J. Aerosp. Eng.*, **9**, 1-22.
- Garnich, M. and Akula, V. (2008), "Review of degradation models for progressive failure analysis of fiber reinforced polymer composites", *Appl. Mech. Rev.*, **62**(1), 010801.
- Icardi, U., Locatto, S. and Longo, A. (2007), "Assessment of recent theories for predicting failure of composite laminates", *Appl. Mech. Rev. ASME*, **60**(2), 76-86.
- Irrhirane, E.H., Abousaleh, M., Echaabi, J., Hattabi M., Saouab, A. and Bensalah, M.O. (2010), "Modeling and simulation of the failure and stiffness degradation of a graphite epoxy in a three Point bending test", *J. Eng. Mater. Tech. ASME*, **132**(3), 1-8.
- Johnson, H.E., Louca, L.A. and Mouring, S.E. (2006), "Damage modeling of large and small scale composite panels subjected to a low velocity impact", HSE Report.
- Khalili, S.M.R., Soroush, M., Davar, A. and Rahmani, O. (2011), "Finite element modeling of low-velocity impact on laminated composite plates and cylindrical shells", *Compos. Struct.*, **93**(5), 1363-1375.
- Menna, C., Asprone, D., Caprino, G., Lopresto, V. and Prota, A. (2011), "Numerical simulation of impact tests on GFRP composite laminates", *Int. J. Impact Eng.*, **38**(8-9), 677-685.
- Minak, G., Ghelli, D., Panciroli, R. and Zucchelli, A. (2009), "Composite tube behavior under low velocity impact", *Mech. Solid. Brazil*, pp. 385-398.
- Sanchez-Saez, S., Barbero, E. and Navarro, C. (2007), "Analysis of the dynamic flexural behavior of composite beams at low temperature", *Compos. Sci. Technol.*, **67**(11-12), 2616-2132.
- Santiuste, C., Sánchez-Sáez, S. and Barbero, E. (2010), "A comparison of progressive-failure criteria in the

- prediction of the dynamic bending failure of composite laminated beams”, *Compos. Struct.*, **92**(10), 2406-2414.
- Sutherland, L.S. and Guedes Soares, C. (2005), “Impact on low fibre-volume, glass/polyester rectangular plates”, *Compos. Struct.*, **68**(1), 13-22.
- Tan, S.C. and Perez, J. (1993), “Progressive failure of laminated composites with a hole under compressive loading”, *Reinf. Plast. Compos.*, **12**(10), 1043-1057.
- Tiberkak, R., Bachene, M., Rechak, S. and Necib, B. (2008), “Damage prediction in composite plates subjected to low velocity impact”, *Compos. Struct.*, **83**(1), 73-82.

CC

Nomenclature

X_T	Tensile strength in fiber direction	E_{xt}	Maximum tensile strain in fiber direction
X_C	Compressive strength in fiber direction	E_{xc}	Maximum compressive strain in fiber direction
Y_T	Tensile strength in transverse direction	E_{yt}	Maximum tensile strain in transverse direction
Y_C	Compressive strength in transverse direction	E_{yc}	Maximum compressive strain in transverse direction
S_{12}	Shear strength in x - y plane	E_{11}	Young modulus in fiber direction
S_{23}	Shear strength in y - z plane	E_{22}	Young modulus in transverse direction
S_{13}	Shear strength in x - z plane	$\mathcal{G}_{12}, \mathcal{G}_{21}$	Poisson's ratio in x - y plane
G_{12}	Shear modulus in x - y plane	$\mathcal{G}_{23}, \mathcal{G}_{32}$	Poisson's ratio in y - z plane
G_{23}	Shear modulus in y - z plane	$\mathcal{G}_{13}, \mathcal{G}_{31}$	Poisson's ratio in x - z plane
G_{13}	Shear modulus in x - z plane	ρ	Density
σ_{ij}	Stress tensor components	ε_{ij}	Strain tensor components